Accounting for genetic interactions is necessary for accurate prediction of extreme phenotypic values of quantitative traits in yeast.

Simon K. G. Forsberg[1], Joshua S. Bloom[2,3,4], Meru J. Sadhu[2,3,4], Leonid Kruglyak[2,3,4] & Örjan Carlborg[1*]

[1]Department of Medical Biochemistry and Microbiology, Uppsala University, Uppsala, Sweden.
[2]Department of Human Genetics, University of California, Los Angeles, Los Angeles, California 90095, USA.
[3]Howard Hughes Medical Institute, University of California, Los Angeles, Los Angeles, California 90095, USA.
[4]Department of Biological Chemistry, University of California, Los Angeles, California 90095, USA.

[*]Correspondence should be addressed to Ö.C. (email: orjan.carlborg@imbim.uu.se).

Experiments in model organisms report abundant genetic interactions underlying biologically important traits, whereas quantitative genetics theory predicts, and data support, that most genetic variance in populations is additive. Here we describe networks of capacitating genetic interactions that contribute to quantitative trait variation in a large yeast intercross population. The additive variance explained by individual loci in a network is highly dependent on the allele frequencies of the interacting loci. Accurate predictions of phenotypes for some multi-locus genotype classes in an epistatic network often require accounting for the interactions. We discuss the implications of these results for attempts to dissect genetic architectures and to predict individual phenotypes and long-term responses to selection.

When the combined phenotypic effect of alleles at two or more loci deviates from the sum of their individual effects, it is referred to as a genetic interaction or epistasis. Most biological traits are regulated by a complex interplay between multiple genes and environmental factors. Despite this underlying complexity, data and theory have shown that it is expected that most of the genetic variance in a population will be additive[1–3]. The apparent contradiction between the complexity of the biological mechanisms that determine quantitative traits, and the observation that most genetic variance seem to be additive, has led to a long-standing debate in genetics: Does the predominant role of the additive genetic variance mean that strictly additive models are always sufficient to describe the relationship between the genotype and the phenotype of an organism[1,4], or could there be added value in explicitly modeling genetic interactions despite the lower levels of epistatic genetic variance[5–8]?

There are some situations where data and theory has suggested that it might be particularly important to account for genetic interactions. One is when the aim is to predict phenotypes of individuals based on their genotype. If interactions lead to extreme phenotypes for some genotypes, and particularly if they are rare, these phenotypes are unlikely to be predicted by additive models. This has, for example, been illustrated for sporulation efficiency in yeast[9]. Another is in the prediction of long-term selection response. Under additivity, both the additive variance and the response are expected to be near constant over the first few generations. As generations proceed, allele-frequencies change to alter the additive variance and consequently the response to selection. This change is more rapid for traits regulated by fewer loci with larger effects than for traits regulated by many loci with smaller effects. It is

known that also genetic interactions can contribute to the additive genetic variance in a population [1,7]. This contribution varies depending on the joint allele-frequencies across all the interacting loci as well as on the types and strengths of the genetic interactions[10,11]. The changes in the additive variance, and hence the response, during ongoing selection is therefore more complex in the presence of genetic interactions. As a result, genetic interactions can make the long-term selection response more dynamic [12,13] and result in a realized response beyond predictions based on the additive genetic effects and allele-frequencies at the individual loci[10,11]. However, as little is known about how prevalent and strong genetic interactions are in real populations, and how much they contribute to the additive variance, it has been difficult to obtain any empirically based conclusions about how influential interactions are expected to be in these situations.

Here we analyze a panel of 4390 yeast recombinant offspring (segregants) from a cross between a lab strain (BY) and a vineyard strain (RM), generated in Bloom, et al. 2015[3]. In this population, each segregant is genotyped for 28,220 SNPs and phenotyped for 20 end-point growth traits. Across these traits, a total of 939 QTL were mapped in a previous study[3], of which 330 were involved in epistatic interactions with at least one other QTL. This dataset presents a unique opportunity to evaluate how allelic combinations across large numbers of loci influence quantitative traits since the individuals are haploids, sample size is large and all allele frequencies are close to 50%. As we will discuss below, we can obtain high confidence estimates of the phenotypes produced by every possible allelic combination across many loci to facilitate in-depth explorations of high-order interactions. Using this data, we show that most traits are determined in part by multiple interacting loci that are part of larger epistatic networks. Further, we also find that the interactions in these networks make large contributions to the additive genetic variances for many traits and that they will bias predictions of individual phenotypes from additive models. We illustrate the impact of these observations by analyzing an individual network in detail, and also by generalizing the results across a large number of additional networks. The potential impact of these findings on prediction of individual phenotypes in personalized medicine, prediction of long-term selection response in breeding and evolution as well as in the interpretation of results from QTL and GWAS studies are discussed.

Results

Many epistatic QTL are part of highly connected networks

Most epistatic QTL in this population interact with one or a few other loci, but a large number of them are involved in pairwise interactions with several other loci[3] [Figure S1]. We visualized the networks for each trait by using the 330 statistically significant epistatic QTL as nodes, and the interactions between them as edges. We selected 15 highly connected networks for further in-depth studies [Figure S2-S12]. These networks contribute to 11 of the 20 studied traits, and each included at least one QTL that interacted with four or more other loci. We refer to QTL with at least four interactions as hubs. Here, only the 105 QTL that directly interacted with at least one such hub were included.

An epistatic network regulating growth in Indoleacetic acid containing medium

Our network-analysis identified a five-locus network regulating growth on medium containing indoleacetic acid (IAA). One QTL in this network interacted in a pairwise manner with the four other loci, and was therefore classified as a hub in this network. We refer to this type of network topology as radial, where the central locus is the hub-QTL, and the other loci

are defined as radial QTLs. Below, we use this network as a case study for an in-depth analysis of the role of genetic interactions.

One genotype at the network hub-QTL hides the phenotypic effects of the radial QTL
The hub-QTL in this network was the individual locus that, in the earlier analysis[3], explained most additive genetic variance for this trait in the population $\left(\frac{\sigma_a^2}{\sigma_p^2} = 11\%\right)$. Here, we first estimated how an allele-substitution at this hub-QTL affects the contributions by the four radial QTL in the network to growth. We found that, when examining only the segregants with the RM allele at the hub-QTL, the four radial loci together only explain 1.2% of the phenotypic variance (σ_p^2), whereas they explain 34% of σ_p^2 among the segregants with the alternative BY allele. The RM allele at the hub-QTL thus hides the phenotypic effects of the four radial QTL, since the growth-decreasing alleles at these loci are silent on the RM genetic background. The BY allele at the hub-QTL on the other hand, allows the genetic variation at the radial QTL to be revealed phenotypically. We refer to this hub-QTL and other loci behaving in this way as genetic capacitors. Also, after removing the contributions by the four known radial QTL, the additive genetic variance was still slightly larger among the segregants with the BY allele (16% vs 13% of σ_p^2), suggesting that the hub-QTL might also moderate the effects of other loci in the genome. To identify such loci, whose effects are larger in the presence of the BY allele at the hub-QTL, we performed a linkage analysis in the group of segregants with the BY hub-QTL allele to reveal a sixth genome-wide significant locus in the radial network.

To clarify how individual alleles, and allelic combinations, in the six-locus network contribute to growth in the IAA containing medium, we estimated the phenotypic means in every multi-locus genotype class. We divided the segregants into 64 groups, each representing one of the possible six-locus allelic combinations for these loci, and then estimated the phenotypic means and variances for each of these classes. Figure 1 visualizes how the RM/BY alleles at the hub-QTL in the network decrease (canalize) and increase (capacitate) the effects of the radial loci by sorting, and coloring, the genotype-values based on the genotype at the hub-QTL. Among the segregants that have the capacitating BY-allele at the hub-QTL (green), the growth is lowest among those that have many IAA-sensitising alleles at the five radial QTL loci. In contrast, among segregants with the canalizing RM-allele at the hub-QTL (pink), there is almost no difference in growth regardless of how many IAA-sensitising alleles they have at the radial loci. The genetic variance is thus considerably higher among the segregants with the capacitating BY allele at the hub QTL.

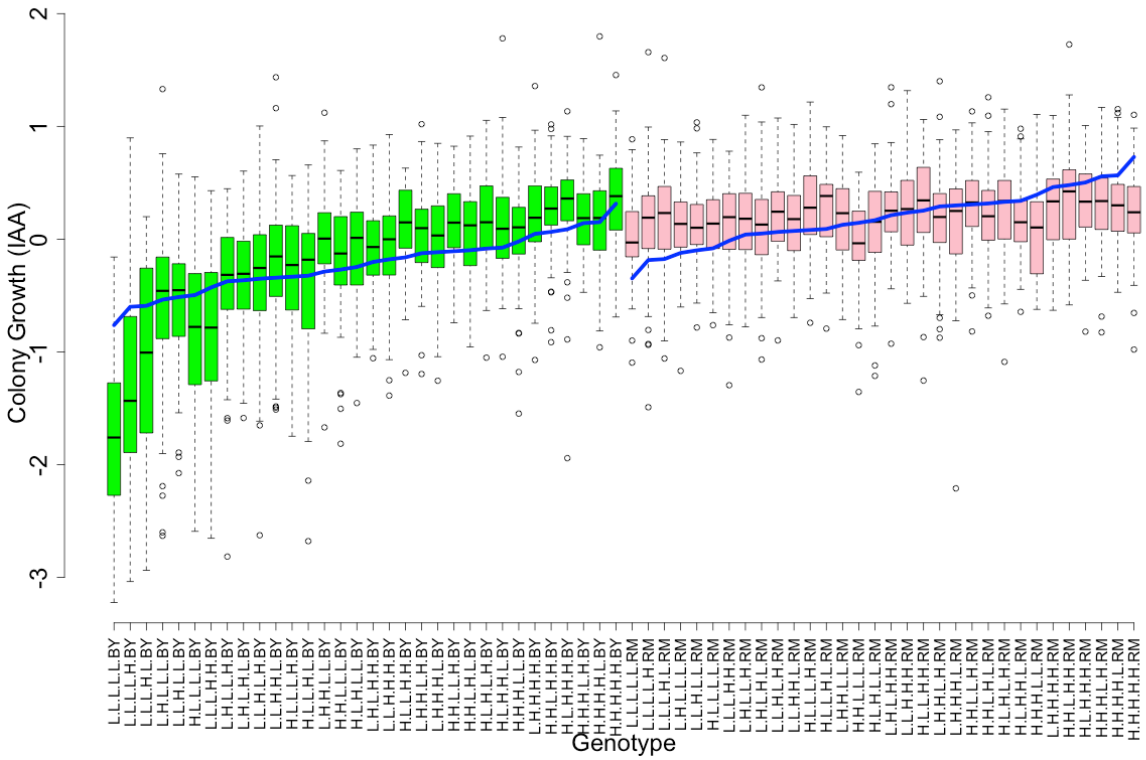

Figure 1. An epistatic network regulates growth on indoleacetic acid containing medium: one genotype at the network hub-QTL hides the phenotypic effects of the radial QTL.
Boxplots illustrating the phenotypic distributions in each of the 64 genotypic classes for the six-locus network. The x-axis indicates the six-locus genotype class, where: RM/BY represent the two alleles at the hub-QTL and L/H the alleles at the five radial QTL. The genotypes with an RM allele at the hub-QTL has less variable (canalized) phenotypes, whereas the genotypes with a BY allele has more variable (capacitated) phenotypes. The L alleles at the radial loci are those that decrease growth on IAA, whereas the H alleles increase growth. The boxes are colored based on the genotype at the hub-QTL, with pink/green representing the RM/BY alleles, respectively. The blue line through the boxes illustrates the predicted phenotypes for the 64 genotype-classes from a linear model assuming that the six loci act additively.

Genetic variance heterogeneity of the hub-locus in the radial network
As illustrated in Figure 1, there is a mean difference in growth between the groups of segregants with BY (green) and RM (pink) alleles at the hub-QTL, which explains why this locus captures much of the additive genetic variance in the population. As shown by the results above, and in Figure 1, there is also a larger phenotypic variability amongst the segregants with the BY allele at the hub-QTL. This genetic variance-heterogeneity is highly significant after accounting for the mean difference between the genotypes[14] ($p < 1{\times}10^{-16}$) and illustrates how the 3-fold higher phenotypic variance associated with the *BY*-genotype (Figure 1) is a result of the allelic interactions.

The growth decreasing alleles at the radial QTL combine their effects in a non-linear fashion
As shown in Figure 1, the five radial QTL show their effects in segregants with the BY allele at the hub-QTL, whereas their effects on the RM genetic background are almost negligible. We dissected this genetic variation further by first dividing the 64 genotype-classes in this network by the genotype at the hub-QTL. Then, we estimated the phenotypic means and

variances for the groups of segregants that, within these two bins, share the same number of IAA-sensitising alleles at the five radial QTL. Figure 2 illustrates that it is only among the segregants with the BY allele at the hub-QTL that the number of growth-decreasing alleles at the radial QTL in the network is correlated with lower growth on IAA. It also shows that the reduction in growth decelerates in a multiplicative, rather than a linear, manner as the number of IAA-sensitising alleles increases among the segregants with the BY allele at the hub-QTL. In other words, among the segregants with the BY allele at the hub-QTL, the effect of having 5 IAA-sensitising alleles is much larger than 5 times the effect of having one IAA-sensitising allele.

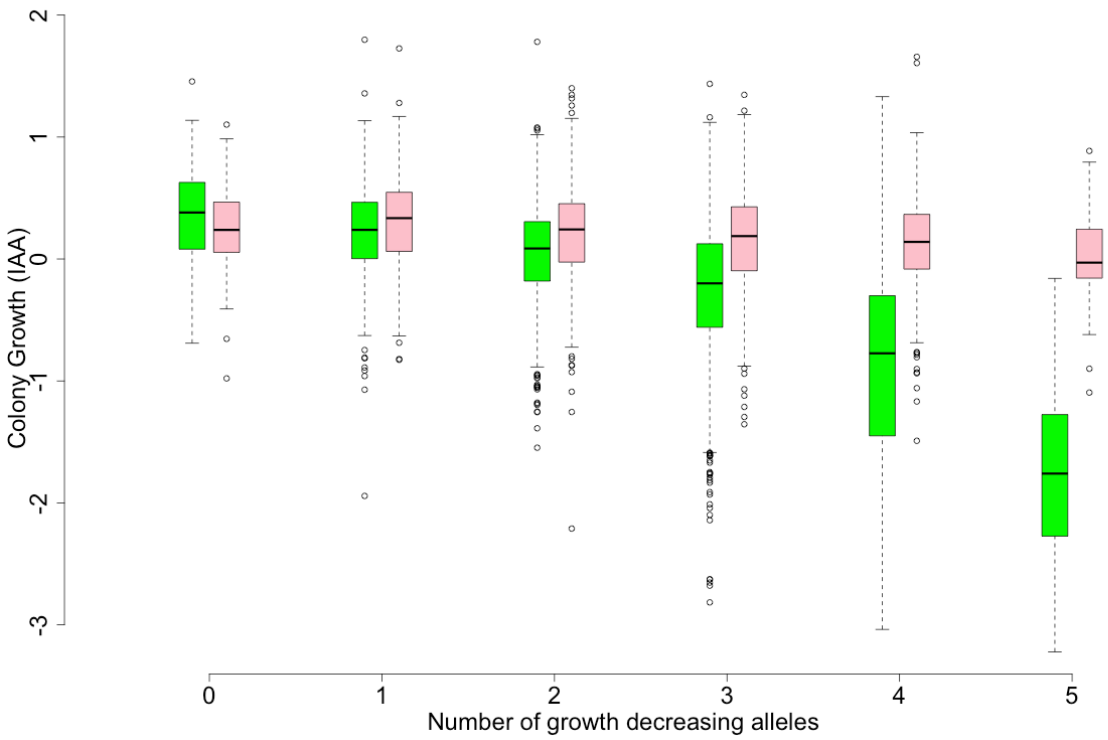

Figure 2. An epistatic network regulates growth on indoleacetic acid containing medium: the growth decreasing alleles at the radial QTL combine their effects in a non-linear fashion

Boxplots illustrating the phenotypic distributions in the groups of segregants with different numbers of growth decreasing alleles at the five radial QTL in the epistatic network. The segregants are divided based on the genotype at the hub-QTL. Segregants carrying the BY (capacitating) allele are shown in green and those with the RM (canalizing) allele are shown in pink. The x-axis gives number of growth decreasing alleles at the radial QTL.

The additive effects and variance-heterogeneity of the hub-QTL depends on the genotypes at the radial loci

Figure 2 also illustrates that the average phenotypes for segregants with the BY allele range from being very similar to that of the segregants with the RM allele at the hub-QTL, when combined with growth-increasing alleles at all five radial QTL, to being considerably lower when combined with several growth-decreasing alleles at the five radial loci. This illustrates several properties of the connection between the functional contribution by the hub-QTL to growth, and how this contribution will be summarized in a statistical, quantitative genetic analysis of a population.

The additive effect of the hub-QTL, as estimated in a quantitative genetic analysis, is the difference in average phenotype between the groups of segregants in the population that carry the BY allele (green) and RM allele (pink) at this locus. In a population where the BY and RM alleles of the hub-QTL segregate, but the radial loci are fixed for IAA-resistant alleles, there will be no, or a very small, difference in the average phenotype between the groups of segregants carrying the RM and BY alleles (the two leftmost boxplots in Figure 2). The hub-QTL will thus have an additive effect close to zero. In a population where the BY and RM alleles segregate, but the radial loci are fixed for IAA-sensitising alleles, there will be a very large difference in average phenotype for the segregants carrying the RM and BY alleles (the two rightmost boxplots in Figure 2). This will result in a very large additive effect of the hub-QTL, resulting from the total sensitising effects of all six loci in the network. The additive effect of this hub-QTL is thus highly dependent on its ability to capacitate the effects of the radial QTL in the network.

The variance-heterogeneity effect of the hub-QTL is the difference in phenotypic variance between the groups of segregants that carry the BY and RM alleles at the hub-QTL. In a population where all six loci segregate, there is a large genetically determined phenotypic variation among the segregants carrying the BY allele at the hub QTL. This since the BY allele capacitates the genetic effects of the radial-QTL as discussed above. The segregants that carry the RM allele are, however, all very similar as the RM allele canalizes the effects of the radial loci. In such a population, there will thus be a large genetic variance-heterogeneity between the BY and RM alleles. In a population fixed for any combination of alleles at the radial loci with less than three growth-decreasing alleles, there is almost no difference in phenotypic variance between the groups of segregants that carry the RM and BY alleles at the hub-QTL. Hence, also the variance-heterogeneity effect at the hub-QTL is highly dependent on the ability of the hub-QTL to capacitate the effects of the radial QTL in the network.

Together, the results illustrate that both the additive, and variance-heterogeneity, effects obtained for the hub-QTL in this network are due to its ability to capacitate the allelic effects of other interacting loci. This network is thus an example of how high-order genetic interactions lead to additivity, and variance-heterogeneity, in quantitative genetic analyses.

The genetic variance explained by the network is highly dependent on the allele frequencies in the analyzed population

The amount of genetic variance associated with a locus depends on its phenotypic effect and on the allele frequencies in the analyzed population[15]. When loci interact, the marginal variance explained by each of the epistatic loci is highly dependent not only on the allele frequency at the locus itself, but also on the frequencies at the interacting loci. The genetic variances explained by the loci in the network affecting growth in IAA containing medium are highly dependent on the allele frequencies at all loci in the network due to the extensive allelic interactions among them. When allele frequencies at all loci are 0.5, as they are in the entire population, the additive variance (σ_a^2) contributed by the network is 26.8%. By contrast, when the BY/RM allele at the hub-QTL is fixed (BY allele frequency 1 or 0), σ_a^2

changes to 36% and 3%, respectively. To generalize this result, we used simulations to create populations with a range of possible combinations of allele frequencies between 0.05 and 0.95 at increments of 0.15 for the six loci in the network and evaluated how stable the genetic variance estimates of the individual loci are with regard to the allele frequencies across the other five loci (see Materials and Methods). We also simulated populations without genetic interactions. The results are summarized in Figure 3 and show that different populations with the same underlying allelic interactions, but with differing allele frequencies for the involved QTLs, can display very different additive genetic variances for the individual loci in a quantitative genetic analysis. The largest variation is observed for the hub-QTL (0 to 58% of σ_p^2). The genetic interactions, however, resulted in much larger variability for all loci (average range: 0 to 31% of σ_p^2), illustrated by low and similar variability (average range: 2 to 6% of σ_p^2) observed for all loci in the simulations under pure additivity (Figure 3).

Accounting for epistasis lead to better predictions of individual phenotypes

Having estimated the phenotypic effect of all allelic combinations for this six-locus network, we next investigated the ability of quantitative genetics models to predict the 64 individual genotype values. This was done by fitting three different quantitative genetics models to this six locus network, including i) additive effects, ii) additive effects and pairwise interactions and iii) additive, pairwise and three-way interactions. The inclusion of interaction terms was based on the Akaike Information Criterion (AIC), and the prediction accuracy was evaluated by cross-validation. The blue line in Figure 1 illustrates the predictions of the phenotypes (genotype values) for all individual six-locus genotype classes obtained with the additive-effects only model. Many of the predictions deviate significantly from the true genotype values, illustrating the difficulty of capturing the effect of the extensive allelic interactions between the hub-QTL and the 5 radial QTL using this model. For segregants with a RM allele at the hub-QTL, some additive model genotype values are overestimates (for segregants with many growth-increasing alleles at the radial QTL) while others are underestimates (for segregants with many growth-decreasing alleles at the radial QTL) of the true genotype values. Further, for segregants with the BY allele at the hub-QTL, the prediction error is in the opposite direction, resulting in underestimates for segregants with many growth-increasing alleles, and overestimates for segregants with many growth-decreasing alleles, at the radial QTL. The additive model also severely underestimates the range of phenotypes amongst the segregants due to the effects of this network, predicting a difference between the most extreme phenotypes of 1.5 σ_p, when the true value is 3.2 σ_p. The prediction error is reduced when interaction terms are included in the model: including significant pairwise interactions removes the prediction error from all but a few predictions (Figure S13B), and including significant three-way interactions removes all significant prediction errors (Figure S13C).

Network hubs often capacitate the effects of many other loci

Our analysis of the network affecting growth in IAA-containing medium showed that the highly connected hub-QTL capacitated the effects of the loci with which it interacted. This capacitation resulted in genetic variance heterogeneity between the BY and RM alleles at the

locus. We next wanted to evaluate whether it is a general trend in the data that loci interacting with multiple other loci, i.e. potential network hubs, are likely to capacitate the effects of loci with which they interact. As genetic capacitation leads to variance-heterogeneity between the genotypes at the capacitor-locus[16,17], we tested this hypothesis by estimating the correlation between the level of variance heterogeneity at the 330 mapped epistatic loci in this population and the number of epistatic interactions they were involved in (Figure S27). This correlation was very strong ($r^2 = 0.64$; $p < 1{\times}10^{-16}$), illustrating that the genetic variance-heterogeneity increases with the number of interactions a locus is involved in. This suggests that more connected (hub) loci are often likely to capacitate the effects of other loci in the genome.

To explore this suggested epistatic capacitation by more connected loci in more detail we looked at all the 15 identified hub-QTLs, present in 15 epistatic networks affecting 11 of the 20 studied traits. We analyzed the effects of these hub-QTLs with an approach similar to the one used for the hub-QTL in the network affecting growth in IAA containing medium. For each of these networks, the set of segregants was divided based on the genotypes at the hub-QTL and the total additive genetic variance estimated in each of these groups. For 12 of the 15 hub-QTLs, there was a significant difference in the fraction of the total variance that was explained by the additive genetic variance $\rho = \frac{\sigma_a^2}{\sigma_a^2+\sigma_e^2}$ between these two groups (range $\left|\rho_{Group1} - \rho_{Group2}\right| = 10\ to\ 42\%$). Together, these results show that the network hub-QTLs revealed in this population, in general, capacitate the effects of many other loci in the genome in a way where one of the hub-QTL alleles acts to capacitate, and the other to canalize, the effects of many loci simultaneously.

Allelic interactions contribute to the additive genetic variance

The large number of genotyped and phenotyped haploid segregants in the analyzed population allowed us to obtain high-confidence estimates of the mean phenotype within every six-locus genotype class (64 in total) for the 15 selected highly connected epistatic networks (range $n = 26\ to\ 117$ segregants per class). This gives the expected mean phenotype (genotype values) within every possible six-locus genotype class. As above with IAA, we then estimated the additive genetic variances and effects in populations simulated based on these estimates, with allele frequencies representing the entire six-locus allele frequency space. This analysis revealed how dependent these estimates are on the types and strengths of allelic interactions observed in this data for more than 100 loci. The estimates were, in general, highly dependent on the allele frequencies of the other loci in the network. In simulations holding the allele frequency of an individual locus constant while varying the allele frequencies of the other loci, we found that the estimated additive genetic variance of the individual locus could range from zero to the largest contribution by any single locus across all networks (Figure 3; Figures S28-S41). A similar variability was observed for the estimates of the additive effect sizes (Figures S42-S56). When similar simulations were performed for completely additive genetic architectures, much less variation was observed in both the variance explained and additive effects (Figures S28-S56). Overall, the estimates of the additive variances were much more variable for epistatic than for additive architectures, with on average a 3-fold (range 1 -

12) increase as measured by the ratio of the standard deviations of the distributions of the estimated variances (Figure 3; Figures S28-S41).

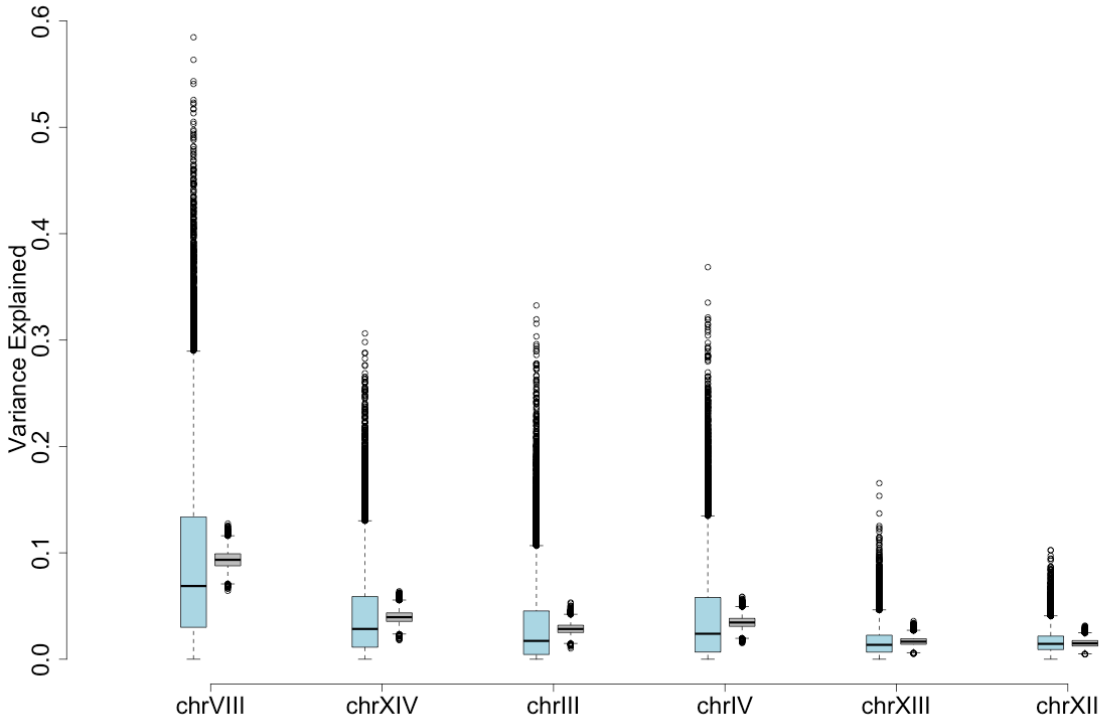

Figure 3. An epistatic network regulates growth on Indoleacetic acid containing medium: The genetic variances explained by the network is highly dependent on the allele-frequencies in the analyzed population *Boxplots illustrating how the additive genetic variances explained by each of the six loci in the network depend on the allele frequencies at the other loci. The distributions are obtained using simulations where the additive genetic variances are estimated for the loci at a fixed allele frequency 0.5, while varying the frequencies at the other 5 loci from 0.05 to 0.95 in increments of 0.15. The light blue boxes on the left represent the variability in the additive genetic variances when simulating populations based on the observed phenotypic means for the allelic combinations in the networks and the grey boxes when simulating based on the phenotypic means predicted using the additive genetic model (Figure 1).*

Phenotypic predictions based on additive models often provide incorrect estimates for extreme genotype values

We fitted statistical quantitative genetic models with and without interactions to the loci in all the 15 most interconnected networks in the same way as was done earlier for the network affecting growth in IAA-containing medium. We used 10-fold cross validation to evaluate the ability of the models to predict the phenotype for every 6-locus genotype class. The models with only additive effects captured much of the phenotypic variance for all these networks (on average 28% of σ_p^2), and adding epistasis to these models only increased the total variance explained marginally (on average 5% of σ_p^2). The additive-only models, however, often resulted in mis-predictions of the mean phenotypes within one or more of the genotype-classes. For 11 of the 15 examined networks, predictions were significantly different from the true values for between one and thirteen of the 64 allele-combinations per network ($p < 10^{-4}$). Including all pairwise interaction terms in the models resulted in accurate predictions

of all genotype values for most networks. Two networks, however, required inclusion of three-way interactions to completely remove prediction errors.

Discussion

The link between the genotype and the phenotype of an organism is immensely complex. Despite this, the relationship between genotype and phenotype in a population can, to a great extent, be captured using models assuming that genes combine their effects in an additive manner. We have here made use of a large experimental yeast cross to identify multi-locus epistatic networks affecting 20 complex traits. For these, we directly estimated the average phenotypes for the groups of segregants that shared the same combinations of alleles for the loci in these epistatic networks. In most networks we identified at least one, but often several, allelic classes where the phenotypes resulting from combining particular alleles deviated significantly from what it would be if the alleles acted additively. This empirically suggests that classic epistasis, as defined by Bateson more than 100 years ago[18], is an important component in the genetic architecture of most complex traits, and we find several striking examples of such epistasis due to allelic interactions between multiple loci in highly interconnected genetic networks.

As illustrated in an earlier study of this population[3], most of the genetic variance for the 20 measured traits is additive. Consistent with this is our observation that reasonable predictions of average phenotypes can be obtained for most multi-locus genotype classes in the epistatic networks based on average allele-substitution effects from additive genetic models. However, at the same time the predictions from the additive models often failed for the allelic combinations with the most extreme phenotypes, and as shown in Figure 1 this misprediction can be very large (1.7 σ_p; Figure 1). This empirically illustrates the importance of designing and analyzing genetic studies using models that capture and predict the features of the underlying genetic architectures that are of greatest relevance for the aim of the study. Regardless of the underlying genetic architecture, additive models will be useful for revealing the genes that contribute most to the phenotypic variance in a particular population and for predicting short-term population-wide response to selection in applications such as animal and plant breeding. On the other hand, models accounting for epistasis are likely to be important for identifying and predicting the effects of combinations of alleles leading to extreme phenotypes in, for example, prediction of disease-risk in individual patients or long-term response to selection where the allele-frequencies of the contributing loci differ from those in the current population.

As shown here and in earlier studies[1,7,19], most genetic variance in a population is expected to be additive even in the presence of extensive epistasis. Due to the lack of empirical knowledge about how common and strong epistasis is in the genetic architecture of complex traits, it is largely unknown how much of the observed additive genetic variance will be contributed by allelic interactions. Here, we analyzed a large experimental yeast population to obtain unique insights about how common and strong multi-locus allelic interactions are in the genetic architectures of multiple quantitative traits. Using these as a basis, we used

simulations to demonstrate that the experimentally observed epistasis would be expected to have a very large influence on both the estimates of the additive genetic effects of the individual loci, and their contributions to the additive genetic variance in populations with various combinations of allele frequencies across these loci. The most striking example was found for growth on medium containing Indoleacetic acid. In this case, the additive variance contributed by the hub in the epistatic network (Figure 1) ranged from explaining no variation at all $\left(\frac{\sigma_a^2}{\sigma_p^2} = 0\right)$, to making the largest contribution by any single locus across all networks $\left(\frac{\sigma_a^2}{\sigma_p^2} = 58\%\right)$, all depending on the allele frequencies of the other 5 loci in the network. Our results are valuable empirical illustrations of how allelic interactions (epistasis) can be the main driver of the additive genetic variance observed in a population, and further, that it is not possible to predict the importance of epistasis in the genetic architecture of a complex trait based on the observed levels of additive and epistatic genetic variance in a population.

Many of the interacting loci in this population were connected into radial epistatic networks where central hub loci interact with multiple other QTLs. We found that this network topology influenced how the loci contributed to the phenotypic variability in the population. For nearly all networks with this topology, the total additive genetic variances were to a great extent determined by the genotype at the hubs. We interpret this as a strong indication that these hub-QTLs are genetic capacitors, i.e. loci with an ability to modify the effects of many other loci in the genome. This type of genetic interactions are, as illustrated here, highly influential for the total level of phenotypic variance displayed in a population as they can both buffer and release standing genetic variation[20,21]. Several well known examples of such genetic capacitors have been studied in molecular detail, including the heat shock protein *HSP90*[22,23] and *EGFR*[24], and examples also exist where this type of genetic architecture has been influential for long-term selection response in vertebrates[10,12]. That radial network architectures around genetic capacitors are common and highly influential for many traits in this population suggests that this type of genetic architecture should be considered in studies of complex traits in yeast, and likely also in other organisms.

It is currently unknown how indoleacetic acid affects yeast fitness, but the discovery of the epistatic network described here may shed some light on its mode of action. The hub-QTL for indoleacetic acid maps to *GPA1*, which is required for the yeast response to mating pheromone. Importantly, although this response is not normally triggered under laboratory growth conditions, as the yeast is not exposed to mating pheromone, the BY allele of *GPA1* causes residual expression of the pheromone response pathway[25,26]. Thus, a model for the capacitance activity of the BY allele of *GPA1* is that indoleacetic acid primarily affects cells with an activated pheromone response pathway. Interacting radial QTLs would then arise if the underlying variants influence either the response to this effect or the activation of the pheromone response pathway by $GPA1_{BY}$. Intriguingly, the radial QTLs include several genes involved in pheromone response. For instance, the radial QTLs contain *MAT,* which dictates which pheromones are expressed or sensed (and is known to interact with *GPA1*)[27], and *VPS34,* which is required for *GPA1*'s activation of the mating pathway[28]. Further work will be required to elucidate the importance of the yeast pheromone response pathway for the fitness effects of indoleacetic acid.

In summary, we show that capacitating genetic interactions are common and strong in the regulation of multiple complex traits in a large experimental yeast population. These results are used to illustrate and discuss how epistasis is expected to affect genotype based prediction of individual phenotypes, long-term selection response, and the inference of genetic architectures using estimates obtained in population-based quantitative genetics analyses. In this way, we empirically show that the role of genetic interactions in complex trait genetics need to be explored beyond quantitative genetic estimates of epistatic genetic variances to understand how they contribute to shaping the phenotypic variability in populations. This is a key fundamental discovery to resolve the long-standing debate in the field about how to approach epistasis in complex trait genetics research.

Methods

The creation of the BYxRM cross, genotyping and phenotyping has previously been described in[2,3]. Additive QTLs were mapped as described in[3]. All analyses were performed using the R framework for statistical computing[29]. All figures were prepared using R.

Inferring epistatic networks

Pairwise epistatic interactions were mapped as in Bloom *et al.*[3]. Networks of epistatic loci were inferred by connecting loci that displayed pairwise interactions. The R-package *igraph*[30] was used to visualize individual networks and to identify network hubs. The GWA analysis for growth on Indole Acetic Acid containing medium among the segregants with the *C*-allele at the hub-locus was performed using the *qtscore* function in the R-package *GenABEL*[31]. The additive genetic variance explained by certain QTLs was calculated as the R^2 from a fixed effect model without interactions.

Estimating average phenotypes for multi-locus genotypes

The average phenotypes were estimated for each of the $2^6 = 64$ possible combinations of alleles for 15 six-locus epistatic networks. Each of these networks had a hub-QTL connected to the other five radial loci by pairwise interactions. On average, $\frac{4390}{64} \approx 69$ segregants are expected in each six-locus genotype class in these networks, allowing confident estimation of the average growth associated with carrying each possible combination of alleles at these loci. Some of the hubs were connected to more than five other loci in the network in the initial network analysis. However, here we only kept the loci with the strongest statistical interaction with the hub-QTL as we could not confidently estimate phenotypes for networks with more than six loci.

Estimation of the genetic variance heterogeneity at individual loci

To analyze the difference in the phenotypic variability between segregants that carry alternative alleles at the epistatic loci, we used a Double Generalized Linear Model (DGLM)[14], as suggested in Rönnegård et al.[16]. This model allowed us to simultaneously model the effects of every locus on the phenotypic mean and variance. We fitted a DGLM with linear predictors for both mean and variance as $y \sim N(X\beta_1, e^{X\beta_2})$ using the R-package

dglm[32], where *y* is the phenotype, *X* is the genotype, β_1 is the effect on the mean, and β_2 is the effect on the variance. Coding the genotypes in *X* as 0 and 1, β_1 will then describe the difference in mean whereas e^{β^2} describes the fold difference in variance between the segregants with alternative alleles at the analyzed locus.

Estimating the capacitating effects of the hub-QTLs in the epistatic networks

We defined QTLs that interacted with more than 4 other loci as hubs. We estimated the capacitating effects of all hub-QTL as follows. For each network containing a hub-QTL, we divided the segregants into two groups based on their genotype at the hub. We then fitted the mixed model $y = X\beta + a + e$ separately for each group. Here, *y* is a column vector containing the phenotypes, *X* is a column vector of ones, β is the overall mean, $b \sim N(0, A\sigma_a^2)$ and $e \sim N(0, \sigma_e^2)$. A is the additive kinship matrix, giving the fraction of the genome shared between each pair of segregants, σ_a^2 is the additive genetic variance captured by the markers, and σ_e^2 is the residual variance. *A* was calculated using the *ibs* function in the R-package GenABEL. We used the function *polygenic*, also from GenABEL, to fit the mixed model. The fraction of additive genetic variance in each group was then calculated as the intra class correlation $\rho = \frac{\sigma_a^2}{\sigma_a^2 + \sigma_e^2}$.

To test the significance of the difference $\rho_1 - \rho_2$ between the two groups of segregants in each network, we performed the following permutation test. For each of the 20 traits, we randomly divided the population into two groups and estimated ρ_1 and ρ_2 in these as described above. This procedure was repeated 1000 times per trait to obtain 20 empirical NULL distributions. The difference $\rho_1 - \rho_2$ between the two groups defined by a hub was considered significant at a multiple testing threshold of $\frac{0.05}{15} \approx 0.003$ when compared to the empirical NULL distribution of the corresponding trait.

Predicting the phenotypes for individual multi-locus genotype classes

For each six-locus epistatic network, we evaluated the phenotypic predictions from three different models, including i) additive effects, ii) additive effects and pairwise interactions and iii) additive, pairwise and three-way interactions. For ii) and iii), we used a backward elimination approach to select which interaction terms to include in the model. Briefly, this approach includes the terms that jointly minimizes the $AIC = 2k - 2ln(L)$, where *k* is the number of estimated parameters and *L* is the maximum likelihood value for the model. We used the R-function *step* in the *stats* package to perform the backward elimination[29]. The predictive performances of the models were then evaluated using 10-fold cross-validation, as implemented in the R-function *CVlm* in the *DAAG* package[33].

Within each of the 64 genotypic classes defined by the six loci in each network, we tested if the CV-residuals significantly deviated from 0 using a t-test. If the deviation was significant at a multiple testing threshold of $\frac{0.05}{64 \times 15} \approx 5.2 \times 10^{-5}$, we considered the predictions to be biased for that particular genotypic class.

Simulations

In the simulations, we used the phenotypic means $\mu_1 \cdots \mu_{64}$ in each of the $2^6 = 64$ classes for each of the 15 six-locus networks, and the total phenotypic variance σ_p^2 for each trait, obtained in the analyses above as a representation of the genetic architectures of these traits. In every individual simulation, we generated populations with the same number of segregants as in the original dataset ($n = 4390$). The number of segregants in each genotype class was determined by the allele frequencies $p_1 \cdots p_6$ at the six loci. For example, the number of observations with genotype *ABcDef*, where the big/small letters indicate the alternative alleles at the six loci, would be $p_1 \times p_2 \times (1 - p_3) \times p_4 \times (1 - p_5) \times (1 - p_6) \times n$. To evaluate the effect of different combinations of allele-frequencies at the loci on the results, we simulated populations with $p_k \in \{0.05, 0.20, 0.35, 0.50, 0.65, 0.80, 0.95\}$, where $k = 1 \cdots 6$. This leads to, in total, 7^6 allele frequency combinations. The phenotypes for each individual in each genotype class are then simulated as $y_k \sim N(\mu_k, \sigma^2)$ and $k = 1 \cdots 64$.

As a comparison, we also simulated populations where the genetic architectures (i.e. the phenotype for each of the 64 multi-locus genotypes) for the 15 networks were given by the predictions obtained from the estimates of a six-locus fixed effect additive model fitted to the respective loci in the experimental population. The linear model used was $y = X\beta + e$, where y is a column vector containing the phenotypes, X is a 4390×7 matrix, the first column consisting of ones and columns 2-7 of the genotypes of the six loci, β is a 1×7 column vector with the intercept and the additive genetic effects, and e is the residual variance. Using this model, predictions $\widehat{\mu_1} \cdots \widehat{\mu_{64}}$ were obtained for each genotype class. The simulations were then performed across the different combinations of allele-frequencies as described above, with phenotypes given by $y_k \sim N(\widehat{\mu_k}, \sigma^2)$.

The additive genetic variance explained by each locus was estimated as the R^2 from the linear model $y = X\beta + e$, fitted to the respective subset of the 7^6 simulated populations where the allele frequency of the locus itself was 0.5 ($p_1 = 0.5$), and the frequency at the other five loci varied in $p_k \in \{0.05, 0.20, 0.35, 0.50, 0.65, 0.80, 0.95\}$, where $k = 2 \cdots 6$. In this model, X is a column vector with the genotype of the locus whose allele frequency is 0.5. The additive genetic variances were estimated in such subsets to analyze the effect of the individual locus across variable genetic backgrounds for the other loci, without the estimates being influenced by changes to the allele frequency of the analyzed locus itself.

Funding

Funding was provided by the Howard Hughes Medical Institute and NIH grant R01 GM102308 (L.K.), F32 GM116318 (M. J. S.) and Swedish Research Council grant 621-2012-4632 (Ö.C.)

Author contributions

Analyses were designed by S.K.G.F., J.S.B., M.J.S., L.K. and Ö.C. Analyses were conducted by S.K.G.F and Ö.C. The manuscript was written by S.K.G.F. and Ö.C. and incorporates comments by J.S.B., M.J.S. and L.K.

References

1. Hill, W. G., Goddard, M. E. & Visscher, P. M. Data and theory point to mainly additive genetic variance for complex traits. *PLoS Genet.* **4,** (2008).
2. Bloom, J. S., Ehrenreich, I. M., Loo, W. T., Lite, T.-L. V. & Kruglyak, L. Finding the sources of missing heritability in a yeast cross. *Nature* **494,** 234–7 (2013).
3. Bloom, J. S. *et al.* Genetic interactions contribute less than additive effects to quantitative trait variation in yeast. *Nat. Commun.* **6,** 8712 (2015).
4. Polderman, T. J. C. *et al.* Meta-analysis of the heritability of human traits based on fifty years of twin studies. *Nat. Genet.* (2015). doi:10.1038/ng.3285
5. Cheverud, J. M. & Routman, E. J. Epistasis and its contribution to genetic variance components. *Genetics* **139,** 1455–61 (1995).
6. Carlborg, O. & Haley, C. S. Epistasis: too often neglected in complex trait studies? *Nat. Rev. Genet.* **5,** 618–625 (2004).
7. Mackay, T. F. C. Epistasis and quantitative traits: using model organisms to study gene-gene interactions. *Nat. Rev. Genet.* **15,** 22–33 (2014).
8. Nelson, R. M., Pettersson, M. E. & Carlborg, Ö. A century after Fisher: time for a new paradigm in quantitative genetics. *Trends Genet.* 1–8 (2013). doi:10.1016/j.tig.2013.09.006
9. Gerke, J., Lorenz, K. & Cohen, B. Genetic interactions between transcription factors cause natural variation in yeast. *Science (80-.).* **323,** 498–501 (2009).
10. Le Rouzic, A., Siegel, P. B. & Carlborg, O. Phenotypic evolution from genetic polymorphisms in a radial network architecture. *BMC Biol.* **5,** 50 (2007).
11. Le Rouzic, A. & Carlborg, Ö. Evolutionary potential of hidden genetic variation. *Trends Ecol. Evol.* **23,** 33–37 (2008).
12. Carlborg, O., Jacobsson, L., Ahgren, P., Siegel, P. & Andersson, L. Epistasis and the release of genetic variation during long-term selection. *Nat. Genet.* **38,** 418–20 (2006).
13. Paixão, T. & Barton, N. H. The effect of gene interactions on the long-term response to selection. *Proc. Natl. Acad. Sci. U. S. A.* **113,** 4422–4427 (2016).
14. Smyth, G. K., Journal, S., Statistical, R. & Series, S. Generalized Linear Models with Varying Dispersion. **51,** 47–60 (1989).
15. Falconer, D. S. & Mackay, T. F. C. Introduction to quantitative genetics. *Harlow: Longman* (1996).
16. Rönnegård, L. & Valdar, W. Detecting major genetic loci controlling phenotypic variability in experimental crosses. *Genetics* **188,** 435–47 (2011).
17. Rönnegård, L. & Valdar, W. Recent developments in statistical methods for detecting genetic loci affecting phenotypic variability. *BMC Genet.* **13,** 63 (2012).
18. Bateson, W. Facts Limiting the Theory of Heredity. *Science (80-.).* **26,** 649–660 (1907).
19. Monnahan, P. J. & Kelly, J. K. Epistasis Is a Major Determinant of the Additive Genetic Variance in Mimulus guttatus. *PLOS Genet.* **11,** e1005201 (2015).
20. Bergman, A. & Siegal, M. L. Evolutionary capacitance as a general feature of complex gene networks. *Nature* **424,** 549–552 (2003).
21. Masel, J. & Siegal, M. L. Robustness: mechanisms and consequences. *Trends Genet.* **25,** 395–403 (2009).
22. Rutherford, S. L. & Lindquist, S. Hsp90 as a capacitor for morphological evolution. *Nature* **396,** 336–342 (1998).
23. Queitsch, C., Sangster, T. a & Lindquist, S. Hsp90 as a capacitor of phenotypic variation. *Nature* **417,** 618–24 (2002).
24. Dworkin, I., Palsson, A., Birdsall, K. & Gibson, G. Evidence that Egfr Contributes to Cryptic Genetic Variation for Photoreceptor Determination in Natural Populations of Drosophila melanogaster. *Curr. Biol.* **13,** 1888–1893 (2003).
25. Yvert, G. *et al.* Trans-acting regulatory variation in Saccharomyces cerevisiae and the role of transcription factors. *Nat. Genet.* **35,** 57–64 (2003).
26. Lang, G. I., Murray, A. W. & Botstein, D. The cost of gene expression underlies a fitness trade-off in yeast. *Proc. Natl. Acad. Sci. U. S. A.* **106,** 5755–60 (2009).
27. Brem, R. B., Storey, J. D., Whittle, J. & Kruglyak, L. Genetic interactions between polymorphisms that affect gene expression in yeast. *Nature* **436,** 701–703 (2005).
28. Slessareva, J. E., Routt, S. M., Temple, B., Bankaitis, V. A. & Dohlman, H. G. Activation of the Phosphatidylinositol 3-Kinase Vps34 by a G Protein ?? Subunit at the Endosome. *Cell* **126,** 191–203 (2006).
29. R Core Team. R: A Language and Environment for Statistical Computing. (2014). at <http://www.r-project.org/>
30. Csárdi, G. & Nepusz, T. The igraph software package for complex network research. *InterJournal*

Complex Syst. **1695,** 1695 (2006).
31. Aulchenko, Y. S., Ripke, S., Isaacs, A. & van Duijn, C. M. GenABEL: an R library for genome-wide association analysis. *Bioinformatics* **23,** 1294–6 (2007).
32. Dunn, P. K. & Smyth, G. K. dglm: Double Generalized Linear Models. (2015). at <http://cran.r-project.org/package=dglm>
33. Maindonald, J. H. & Braun, W. J. DAAG: Data Analysis and Graphics Data and Functions. (2015). at <http://cran.r-project.org/package=DAAG>